

ChemComm

Accepted Manuscript



This is an *Accepted Manuscript*, which has been through the Royal Society of Chemistry peer review process and has been accepted for publication.

Accepted Manuscripts are published online shortly after acceptance, before technical editing, formatting and proof reading. Using this free service, authors can make their results available to the community, in citable form, before we publish the edited article. We will replace this *Accepted Manuscript* with the edited and formatted *Advance Article* as soon as it is available.

You can find more information about *Accepted Manuscripts* in the [Information for Authors](#).

Please note that technical editing may introduce minor changes to the text and/or graphics, which may alter content. The journal's standard [Terms & Conditions](#) and the [Ethical guidelines](#) still apply. In no event shall the Royal Society of Chemistry be held responsible for any errors or omissions in this *Accepted Manuscript* or any consequences arising from the use of any information it contains.

Hydrogen-bonded clusters of ferrocenecarboxylic acid on Au(111).

Rebecca C. Quardokus,^a Natalie A. Wasio,^a John A. Christie,^a Kenneth W. Henderson,^a Ryan P. Forrest,^a Craig S. Lent,^b Steven A. Corcelli,^a and S. Alex Kandel^{*a}

Self-assembled monolayers of ferrocenecarboxylic acid (FcCOOH) contain two fundamental units, both stabilized by intermolecular hydrogen bonding: dimers and cyclic five-membered catemers. At surface coverages below a full monolayer, however, there is significantly more varied structure that includes double-row clusters containing two to twelve FcCOOH molecules. Statistical analysis shows a distribution of cluster sizes that is sharply peaked compared to a binomial distribution. This rules out simple nucleation-and-growth mechanisms of cluster formation, and strongly suggests that clusters are formed in solution and collapse into rows when deposited on the Au(111) surface.

Self-assembly of molecules onto solid surfaces can produce structures unlike those present in bulk crystals of the same molecules. Strong, local interactions with the substrate can drive molecular ordering, but even in the absence of these, intermolecular interactions can be modulated as adsorbates are confined to two dimensions. The kinetics of monolayer formation—including mobility of adsorbed species and potential exchange processes with solution—also must be considered.

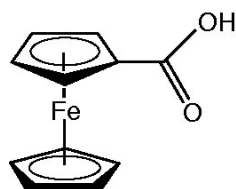


Fig. 1 Molecular structure of ferrocenecarboxylic acid (FcCOOH).

Carboxylic acid dimerization through hydrogen bonding is a common motif exploited in surface self-assembly, and molecules with multiple COOH groups can form ordered two-dimensional networks. Examples include the linear chains present in terephthalic acid monolayers on gold,¹ as well as “chicken wire” lattice formed by connected six-membered rings of trimesic acid on graphite² and gold³ surfaces. Linear catemers, where any given carboxylic acid accepts a hydrogen bond from one neighbor and donates to another, are an alternate structure.^{4,5} It is uncommon for both dimers and

catemers to coexist, though tetrafluorophthalic acid aggregates as both catemers and dimers⁴, and cyheptamide can be transformed from a catemeric crystal structure to a dimeric crystal structure through a heating and cooling process.⁶

Ferrocenecarboxylic acid, shown in Figure 1, is known to have a hydrogen-bonded dimeric solid state structure.⁷ However, monolayers of FcCOOH on Au(111) have a complex structure composed of both dimers and five-membered rings, forming the basis for self-assembly into a two-dimensional quasicrystal.⁸ While dimers and pentamers are the most prominent features in experimental scanning tunneling microscopy (STM) images, some smaller and larger clusters are also observed, particularly in areas with submonolayer coverage. In this Communication, we characterize these clusters more quantitatively, finding a predominance of 5-, 6-, and 8-molecule clusters. We believe that the atypical conditions during the pulse-deposition process—including high concentrations and low temperatures present in rapidly drying droplets—could potentially be responsible for the formation of these clusters, which may not be present under normal laboratory conditions.

The synthesis of FcCOOH has been reported previously.⁸ A 20 mM solution of FcCOOH in benzene was prepared in an argon-purged glovebox. Microliters of solution were deposited by opening a 0.5 mm orifice for 0.5 ms at room temperature via a pulsed-solenoid valve^{9–15} into a preparatory vacuum chamber (10^{-7} Torr) containing a gold-on-mica substrate (Agilent Technologies). Three pulses were deposited on the gold surface. The pressure in the vacuum chamber was allowed to recover between pulses. Prior to deposition the gold was cleaned with two rounds of argon sputtering (2×10^{-5} Torr at 20.0 mA for 20 minutes) and annealing (578 K for 20 minutes). After deposition the sample was immediately moved into ultra-high vacuum ($< 3 \times 10^{-10}$ Torr) and cooled to 77 K prior to imaging with a low-temperature ultra-high-vacuum scanning tunneling microscope (LT-UHV STM from Omicron NanoTechnology).

Most of the sample area imaged in Figure 2a shows a high packing density of cyclic pentamers (shaded red, enlarged portion shown in Figure 2b). Dimers pack between the pentamers and are oriented with the ferrocene cyclopentadienyl (Cp) rings perpendicular to the surface, making them less visible. Some double-rowed clusters are also visible packed among the dimers and pentamers. The overall structure matches that observed in reference 8, and is characterized by a mix of quasicrystalline and periodic structures.

^a Department of Chemistry and Biochemistry, University of Notre Dame, Notre Dame, IN, USA. Tel: 1 574 631 7837; E-mail: skandel@nd.edu

^b Department of Electrical Engineering, University of Notre Dame, Notre Dame, IN, USA.

In between areas with tightly packed pentamers, Figure 2a shows small areas of tightly packed dimers (shaded green, enlarged portion shown in Figure 2c) and areas of disperse FcCOOH structures (shaded blue, enlarged portion shown in Figure 2d). Herringbone reconstruction of the Au(111) surface remains intact and is visible under the tightly packed dimers in Figure 2a. While pentagonal clusters are still present in areas with submonolayer coverage, there is a wider range of features present. This is shown at higher resolution in the similar area imaged in Figure 3. In addition to a cyclic pentamer, clusters with double-row structures containing 4 to 9 molecules are highlighted, and are responsible for the majority of the features that unambiguously appear to be FcCOOH molecules. Dimmer, disordered structure might result from FcCOOH in different orientations, but is more likely due to the presence of some coadsorbed benzene solvent, which remains on the surface after the pulse deposition process.^{16,17}

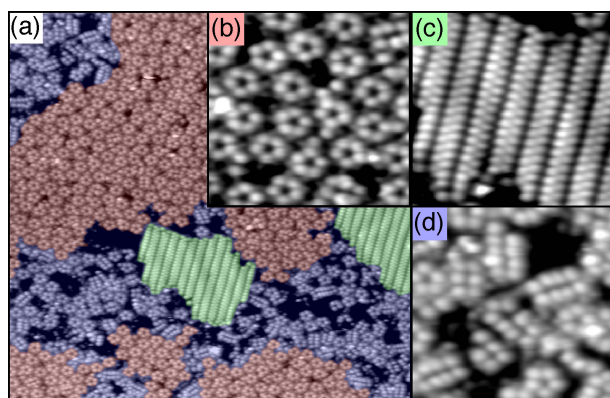


Fig. 2 (a) $620 \text{ \AA} \times 600 \text{ \AA}$, FcCOOH clusters with aperiodic pentamer packing (shaded red, with (b) enlarged to show detail), tightly packed dimers (shaded green, (c)), and loosely packed clusters (shaded blue, (d)). The image was scanned with a tunneling current of 10 pA and a bias voltage of 1.0 V. Panels (b)–(d) each display an area of $105 \text{ \AA} \times 100 \text{ \AA}$.

The formation of hydrogen-bonded dimers and the organization of these dimers into rows is characteristic of surface-adsorbed carboxylic acids.¹⁸ In contrast, assembly into cyclic pentamers is, thus far, unique to FcCOOH. Furthermore, while the double-row clusters in Figure 3 might be simply interpreted as rows of FcCOOH dimers, this explanation falls short for a number of reasons. First, clusters of any particular size can appear in a range of configurations, as shown in Figure 4. The odd-numbered clusters (containing 5, 7, and 9 molecules) have vacancies in one row not only at the ends of the cluster, but also in the middle, showing that dimerization is incomplete. Second, the inter-row spacing is not constant; this is visible in Figure 4 to some extent in panels (e) and (f), and markedly in panel (d). Finally, the distribution of cluster sizes is strongly peaked, with clusters containing more than 10

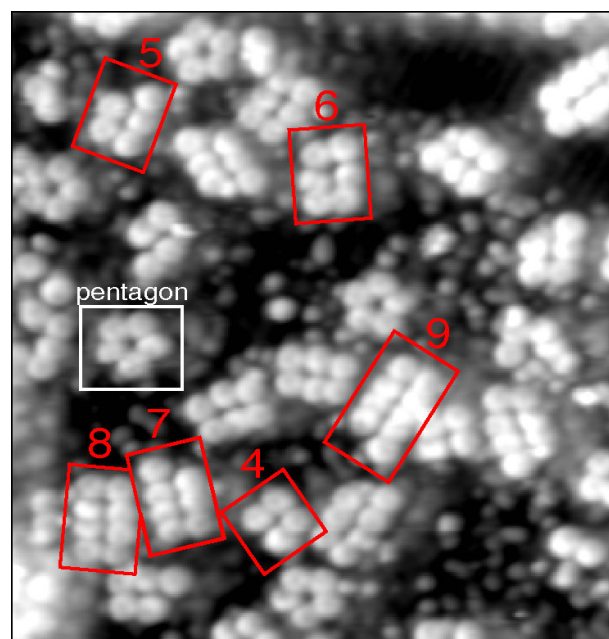


Fig. 3 $185 \text{ \AA} \times 190 \text{ \AA}$, Examples of 4–9-membered groups shown in the red boxes; the white box is around a pentagonal five-membered ring. The image was scanned with a tunneling current of 10 pA and a bias voltage of 1.5 V

molecules virtually nonexistent.

The distribution of cluster sizes was measured using 14 STM images covering 6200 \AA^2 of the surface. The analysis focused on clusters having a double-row geometry, and regular pentagons (white box in Figure 3) and other agglomerations were excluded, as were dimers. 1045 clusters containing 3 and 12 FcCOOH molecules were observed, ranging in size from 2 to 6 rows; no 7-row or larger clusters were found.

A histogram of observed FcCOOH cluster sizes is shown (red points) in Figure 5. While we cannot rule out complex multi-body interactions on the surface (see, e.g., reference 19), most simple surface growth models treat the addition of each molecule as an independent event, necessarily resulting in a binomial distribution of cluster sizes. The best fit to a binomial distribution (blue line) is very poor. A statistical growth process cannot reproduce key features of the experimentally observed data: the sharp peak in cluster sizes with 5, 6, or 8 molecules, the dip in 7-molecule clusters (less common than either 6- or 8-mers), and the sudden drop-off in frequency for all clusters with more than 8 molecules. A ripening process where the units added were dimers instead of monomers also cannot explain the data, as a similar attempt to describe the even-numbered cluster sizes via comparison to a binomial distribution results in a statistically worse fit.

A possible explanation is that small surface-adsorbed clusters are more thermodynamically stable. This was shown in

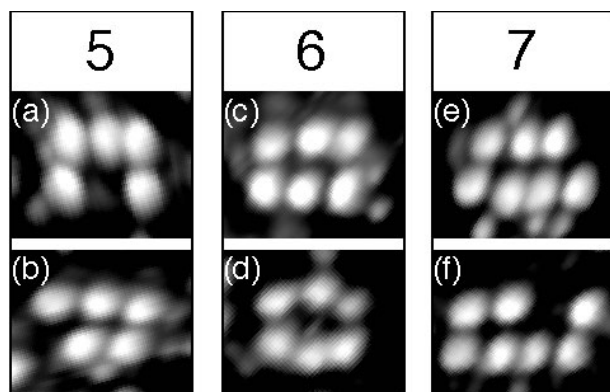


Fig. 4 (a)–(f) $30 \text{ \AA} \times 25 \text{ \AA}$, Examples of variations of 5, 6, and 7 membered clusters. (a),(b),(c),(e), and (f) were scanned with a tunneling current of 10 pA and a bias voltage of -0.5 V . (d) was scanned at 10 pA and 1.0 V .

experiments with 1-nitronaphthalene on Au(111), which determined that the molecules form magic clusters (groups of ten) due to intermolecular forces and substrate effects.²⁰ Such a phenomenon is less likely to produce the range of sizes and shapes that we observe here. Substrate effects also seem to be weak: the gold lattice does not influence the direction of isolated pentamers, and cannot produce the fivefold symmetries seen in the dense pentamer/dimer regions.⁸

Instead, we propose that FcCOOH clusters are forming in solution before adsorption onto the surface, and that the size distribution in Figure 5 derives from the thermodynamic stability of different-sized solvated clusters. There is some experimental evidence that other carboxylic acids form trimers or larger clusters in solution.^{21,22} The pulse-deposition process used to deposit FcCOOH on the surface involves rapid drying of solvent, as the sample is exposed to microliter-sized droplets of solution that are released into vacuum via half-millisecond pulses of a solenoid valve. This likely creates conditions of concentration and temperature that are not accessible through other deposition methods.¹⁴ In particular, even though FcCOOH is sparingly soluble in benzene, we expect high concentrations to occur at some point in the non-equilibrium conditions produced by the drying process.^{23–25} These concentrations would then encourage the formation of solution-phase catemers. The choice of benzene as a solvent removes the possibility of strong solute-solvent hydrogen bonding, and benzene may further encourage agglomeration because solution-phase intermolecular self assembly can be influenced by the polarity of the solvent.²⁶

Five-membered rings are stabilized by the C–H–O hydrogen bonding between the carboxylic acid and the hydrogen on the Cp ring as well as C–H interactions with the π electrons of the neighboring Cp rings, and for clusters constrained to be planar as a result of surface adsorption, electronic structure



Fig. 5 A histogram of FcCOOH cluster sizes (red) observed in STM images of low-coverage areas. The poor fit to a binomial distribution (blue) shows the process is not statistical.

calculations show enhanced stability for pentamers compared to dimers or other cyclic clusters.⁸ In solution, however, the availability of a third dimension will likely broaden the range of stable cyclic structures. For non-planar rings, however, surface adsorption will induce strain, which potentially relaxes through collapse into double-row clusters such as those shown in Figure 3. The pulse-deposition process took place at room temperature, but the samples were imaged at 77 K . It is possible that the clusters were frozen in place after deposition, and that post-annealing or room-temperature experiments would cause the clusters to rearrange on the surface which may give more insight into the causation for cluster formation and the interesting statistical distribution of cluster sizes.

The experimental results here primarily concern the double-row clusters, which we conclude are not dimer rows formed through surface ripening, and which we propose are the result of FcCOOH aggregation in solution before surface deposition. While the data do not directly address the formation of cyclic pentamers, the observation of isolated clusters makes it likely that they, too, can be created in solution prior to adsorption. Because quasicrystallinity in FcCOOH monolayers relies on the formation of these cyclic pentamers, it may derive as much from the non-equilibrium conditions present during pulse deposition as it does from the unusual hydrogen bonding that stabilizes the pentameric structure.

References

- 1 S. Clair, S. Pons, A. Seitsonen, H. Brune, K. Kern and J. Barth, *J. Phys. Chem. B*, 2004, **108**, 14585–14590.

REFERENCES

REFERENCES

- 2 S. Griessl, M. Lackinger, M. Edelwirth, M. Hietschold and W. Heckl, *Single Mol.*, 2002, **3**, 25–31.
- 3 Y. Ishikawa, A. Ohira, M. Sakata, C. Hirayama and M. Kunitake, *Chem. Commun.*, 2002, 2652–2653.
- 4 G. M. Frankenbach and M. C. Etter, *Chem. Mat.*, 1992, **4**, 272–278.
- 5 L. Leiserowitz, *Acta Crystallogr. Sect. B-Struct. Commun.*, 1976, **32**, 775–802.
- 6 A. J. Florence, K. Shankland, T. Gelbrich, M. B. Hursthouse, N. Shankland, A. Johnston, P. Fernandes and C. K. Leech, *Crystengcomm*, 2008, **10**, 26–28.
- 7 F. A. Cotton and A. H. Reid, *Acta Crystallogr. Sect. C-Cryst. Struct. Commun.*, 1985, **41**, 686–688.
- 8 N. A. Wasio, R. C. Quardokus, R. P. Forrest, C. S. Lent, S. A. Corcelli, J. A. Christie, K. W. Henderson and S. A. Kandel, *Nature*, 2014, **507**, 86+.
- 9 S. Guo and S. A. Kandel, *J. Chem. Phys.*, 2008, **128**, 014702.
- 10 T. Kanno, H. Tanaka, T. Nakamura, H. Tabata and T. Kawai, *Jpn. J. Appl. Phys.*, 1999, **38**, L606–L607.
- 11 R. Bernard, V. Huc, P. Reiss, F. Chandezon, P. Jegou, S. Palacin, G. Dujardin and G. Comtet, *J. Phys.: Condens. Matter*, 2004, **16**, 7565–7579.
- 12 L. Grill, I. Stass, K. H. Rieder and F. Moresco, *Surf. Sci.*, 2006, **600**, L143–L147.
- 13 Y. Shirai, A. J. Osgood, Y. M. Zhao, K. F. Kelly and J. M. Tour, *Nano Lett.*, 2005, **5**, 2330–2334.
- 14 Y. Terada, B. K. Choi, S. Heike, M. Fujimori and T. Hashizume, *Nano Lett.*, 2003, **3**, 527–531.
- 15 Y. Terada, B. K. Choi, S. Heike, M. Fujimori and T. Hashizume, *J. Appl. Phys.*, 2003, **93**, 10014–10017.
- 16 D. Zhong, K. Wedeking, T. Bloemker, G. Erker, H. Fuchs and L. Chi, *ACS Nano*, 2010, **4**, 1997–2002.
- 17 R. C. Quardokus, N. A. Wasio, R. P. Forrest, C. S. Lent, S. A. Corcelli, J. A. Christie, K. W. Henderson and S. A. Kandel, *Phys. Chem. Chem. Phys.*, 2013, **15**, 6973–6981.
- 18 B. Xu, B. Varughese, D. Evans and J. Reutt-Robey, *J. Phys. Chem. B*, 2006, **110**, 1271–1276.
- 19 S. Whitelam, I. Tamblyn, T. K. Haxton, M. B. Wieland, N. R. Champness, J. P. Garrahan and P. H. Beton, *Phys. Rev. X*, 2014, **4**, 011044.
- 20 M. Bohringer, K. Morgenstern, W. D. Schneider, R. Berndt, F. Mauri, A. De Vita and R. Car, *Phys. Rev. Lett.*, 1999, **83**, 324–327.
- 21 T. Nakabayashi and N. Nishi, *J. Phys. Chem. A*, 2002, **106**, 3491–3500.
- 22 M. Tjahjono, S. Cheng, C. Li and M. Garland, *J. Phys. Chem. A*, 2010, **114**, 12168–12175.
- 23 M. Faustini, C. Boissiere, L. Nicole and D. Grosso, *Chem. Mater.*, 2014, **26**, 709–723.
- 24 E. Rabani, D. Reichman, P. Geissler and L. Brus, *Nature*, 2003, **426**, 271–274.
- 25 V. Palermo and P. Samori, *Ang. Chem. Intl. Ed.*, 2007, **46**, 4428–4432.
- 26 M. R. Molla, D. Gehrig, L. Roy, V. Kamm, A. Paul, F. Laquai and S. Ghosh, *Chem.-Eur. J.*, 2014, **20**, 760–771.